

# Holographic Approach to Deep Inelastic Scattering at Small- $x$ at High Energy

---

**Chung-I Tan\***

*Brown University, Providence, RI 02912, USA*

*E-mail: [tan@het.brown.edu](mailto:tan@het.brown.edu)*

**R. C. Brower**

*Boston University, Boston MA 02215, USA*

*E-mail: [brower@bu.edu](mailto:brower@bu.edu)*

**Marko Djurić**

*Universidade do Porto, 4169-007 Porto, Portugal*

*E-mail: [djuric@fc.up.pt](mailto:djuric@fc.up.pt)*

**Timothy Raben**

*Brown University, Providence, RI 02912, USA*

*E-mail: [traben13@gmail.com](mailto:traben13@gmail.com)*

We focus on a holographic approach to DIS at small- $x$  in high energy where scattering is dominated by exchanging a Reggeized Graviton in  $AdS_5$ . We emphasize the importance of confinement, which corresponds to a deformation of  $AdS_5$  geometry in the IR. This approach provides an excellent fit to the combined HERA data at small  $x$ . We also discuss the connection of Pomeron/Odderon intercepts in the conformal limit with anomalous dimensions in strong coupling.

*XXIII International Workshop on Deep-Inelastic Scattering,  
27 April - May 1 2015  
Dallas, Texas*

---

\*Speaker.

**Introduction:** AdS/CFT correspondence [1, 2], a conjectured duality between a wide class of gauge theories in  $d$ -dimensions and string theories on asymptotically  $AdS_{d+1}$  product spaces, can be used to study high energy scattering processes in the non-perturbative strong coupling limit. It has been shown, in a holographic or AdS/CFT dual description for QCD, the Pomeron can be identified with a reggeized Graviton in  $AdS_5$  [3, 4] and, similarly, an Odderon as a reggeized anti-symmetric Kalb-Ramond  $B$ -field [5, 6].

In the most robust example, 4 dimensional  $\mathcal{N} = 4$  Super Yang Mills theory, in the limit of large 't Hooft coupling  $\lambda = g_s N_c = g_{ym}^2 N_c$ , is believed to correspond to a limit of type IIB string theory in  $d = 10$ . This identification partially relies on the conformal invariance of the former, but is believed to withstand deformation. The geometry on the string side is a negatively curved space times a sphere,  $AdS_5 \times S^5$ , having Poincare metric  $ds^2 = \frac{R^2}{z^2} [dx^\mu dx_\mu + dz^2] + R^2 d\Omega_5$ , with the conformal group as its isometry. The dual description allows moving from the weak to the strong coupling, with the bulk coordinate  $z$  serving as a length scale, ( $z$  small for UV and  $z$  large for IR.)

It is important to note that conformal invariance is broken for QCD, with a non-zero beta-function, leading to logarithmic running for  $g_{ym}$  at UV and confinement in IR. Nevertheless, approximate conformal invariance remains meaningful, e.g., in perturbative treatment in the UV limit, whereas confinement in the IR limit is crucial in addressing non-perturbative physics. It is thus necessary to deform the metric

$$ds^2 \rightarrow e^{2A(z)} [dx^\mu dx_\mu + dz^2] + R^2 d\Omega_5 \quad (1)$$

where  $A(z) \simeq -\log z$  in UV ( $z = 0$ ) and deviates away from the conformal limit as  $z$  increases in order to account for confinement<sup>1</sup>. Under this ‘‘asymptotic  $AdS$ ’’ setting, it is possible to provide a unified treatment of both perturbative and non-perturbative physics at high energy.

This novel dual approach has been successfully applied to the study of HERA data [7], both for DIS at small- $x$  [10, 11, 12, 13] and for deeply virtual Compton scattering (DVCS) [14]. More recently, this treatment has also been applied to the study of diffractive production of Higgs at LHC [15] as well as other near forward scattering processes [16]. In this talk, we first describe ‘‘Pomeron-Graviton’’ duality and its application to deep inelastic scattering (DIS) at small- $x$ . We next turn to the issue of confinement and in particular the Pomeron singularity in a soft-wall background. We also discuss Pomeron and Odderon intercepts in the conformal limit and their relation to the anomalous dimensions.

**Pomeron-Graviton Duality:** It can be shown for a wide range of scattering processes that the amplitude in the Regge limit,  $s \gg t$ , is dominated by Pomeron exchange, together with the associated  $s$ -channel screening correction, e.g., via eikonalization. In this representation, the near-forward amplitude can be expressed in terms of a Fourier transform over the 2-d transverse (impact parameter) space,  $A(s, t) = 2is \int d^2b e^{i\vec{q}\cdot\vec{b}} \{1 - e^{i\chi(s, \vec{b})}\}$  where  $\chi(s, \vec{b})$  is the eikonal. To first order in  $\chi$ , one has  $A(s, 0) \simeq 2s \int d^2b \chi(s, b) \sim s^{j_0}$  where  $j_0$  is the Pomeron intercept. Traditionally, Pomeron has been modeled at weak coupling using perturbative QCD; in lowest order, a bare Pomeron was first identified as a two gluon exchange, corresponding to a Regge cut in the  $J$ -plane at  $j_0 = 1$ . Going beyond the leading order by summing generalized two gluon exchange diagrams, led to the so-called BFKL Pomeron. The position of this  $J$ -plane cut is at  $j_0 = 1 + \log(2)\lambda/\pi^2$ , recovering the two-gluon cut in the  $\lambda \rightarrow 0$  limit. In

<sup>1</sup>One useful approach is to introduce a sharp cutoff, the so-called hardwall model. Another approach leading to analytic treatment is the so-called softwall model, which we shall turn to shortly.

a holographic approach, the weak coupling Pomeron is replaced by the ‘‘Regge graviton’’ in AdS space, as formulated by Brower, Polchinski, Strassler and Tan (BPST) [3, 4]. The BPST Pomeron contains both the hard component due to near conformality in the UV and the soft Regge component in the IR. To first order in  $1/\sqrt{\lambda}$ , the intercept moves from  $j = 2$ , appropriate for a graviton, down to  $j_0 = 2 - 2/\sqrt{\lambda}$ . In

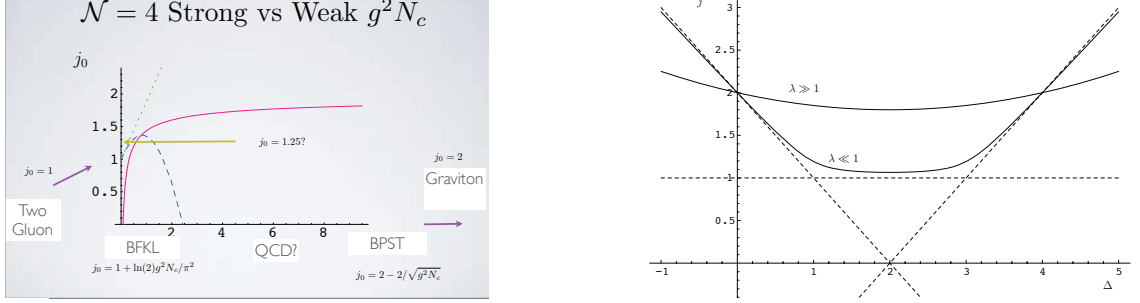


**Figure 1:** On the left, (a), intercept as a function of  $\lambda$  for the BPST Pomeron (solid red) and for BFKL (dotted and dashed to first and second order in  $\lambda$  respectively). On the right, (b), the conformal invariant  $\Delta - j$  curve which controls both anomalous dimensions and the Pomeron intercept.

Fig. 1 a, we compare the BPST Pomeron intercept with the weak coupling BFKL intercept for  $\mathcal{N} = 4$  YM as a function of 't Hooft coupling  $\lambda$ . A typical phenomenological estimate for this parameter for QCD is about  $j_0 \simeq 1.25$ , which suggests that the physics of diffractive scattering is in the cross over region between strong and weak coupling. A corresponding treatment for Odderons has also been carried out [17].

In a holographic approach, the transverse space  $(\vec{b}, z)$  is 3 dimensional, where  $z \geq 0$  is the warped radial 5th dimension. The near-forward elastic amplitude again has the eikonal form [4, 8, 9],

$$A(s, t) = 2is \int d^2b e^{i\vec{q}\cdot\vec{b}} \int dz dz' P_{13}(z) \{1 - e^{i\chi(s, b, z, z')}\} P_{24}(z'). \quad (2)$$

where  $t = -q_{\perp}^2$ . For hadron-hadron scattering,  $P_{ij}(z) = \sqrt{-g(z)}(z/R)^2 \phi_i(z) \phi_j(z)$  involves a product of two external normalizable wave functions for the projectile and the target respectively. Expanding in  $\chi(s, b, z, z')$ , to first order, it is seen that the eikonal function is related to a BPST Pomeron kernel in a transverse  $AdS_3$  representation,  $\mathcal{K}(s, b, z, z')$ , with  $\chi(s, b, z, z') = \frac{g_0^2}{2s} \left(\frac{R}{zz'}\right)^2 \mathcal{K}(s, b, z, z')$ .

**Holographic Treatment of DIS and HERA Data:** A unifying feature for the holographic map is factorization in the AdS space. Because of factorization, this approach can now be applied to all DIS cross sections since they can be related to the Pomeron exchange amplitude via the optical theorem,  $\sigma = s^{-1} \text{Im}A(s, t = 0)$ . For DIS, states 1 and 3 are replaced by currents, and we can simply replace  $P_{13}$  by product of the appropriate unnormalized wave-functions. In the conformal limit,  $P_{13}$  was calculated in [18] in terms of Bessel functions, so that, to obtain  $F_2$ , we simply replace in (2),  $P_{13}(z) \rightarrow P_{13}(z, Q^2) = (Q^2 z) [K_0^2(Qz) + K_1^2(Qz)]$ . (Similarly, for  $F_1$ , one has  $P_{13}(z, Q^2) = (Q^2 z) K_1^2(Qz)$ .) With this substitution, one has, e.g.,  $F_2 = \frac{Q^2}{4\pi\alpha_{em}} (\sigma_T + \sigma_L) = \frac{Q^2}{4\pi\alpha_{em}s} [\text{Im}A(s, 0)_T + \text{Im}A(s, 0)_L]$ . When expanded to first order in  $\chi$ , Eq. (2) provides the contribution to  $F_2$  from a single Pomeron, i.e., the BPST kernel,  $\mathcal{K}(s, b, z, z')$ .

The momentum-space BPST kernel in the  $J$ -plane,  $G_j(t, z, z')$ , obeys a Schrödinger equation on  $AdS_3$  space, with  $j$  serving as eigenvalue for the Lorentz boost operators  $M_{+-}$ . In the conformal limit,

it takes on a simple form,  $G_j(t, z, z') = \int_0^\infty \frac{dq^2}{2} \frac{J_{\tilde{\Delta}(j)}(zq) J_{\tilde{\Delta}(j)}(qz')}{q^2 - t}$ , with  $\tilde{\Delta}(j) = \Delta(j) - 2$ , where

$$\Delta(j) = 2 + \lambda^{1/4} \sqrt{2(j - j_0)} \quad (3)$$

is the conformal  $\Delta - j$  curve shown in Fig. 1b. The full Pomeron kernel can then be obtained via an inverse Mellin transform. In the mixed-representation, one has  $K(s, b, z, z') \sim - \int \frac{dj}{2\pi i} \tilde{s}^j \frac{e^{-i\pi j + 1}}{\sin \pi j} \frac{e^{(2-\Delta(j))\eta}}{\sinh \eta}$  where  $\cosh \eta$  is the chordal distance in  $AdS_3$ . By integrating over  $\vec{b}$ , one obtains for the imaginary part of the Pomeron kernel at  $t = 0$ ,  $\text{Im } \mathcal{H}(s, t = 0, z, z') \sim \frac{s j_0}{\sqrt{\pi \mathcal{D} \log s}} e^{-(\log z - \log z')^2 / \mathcal{D} \log s}$ , which exhibits diffusion in the ‘‘size’’ parameter  $\log z$  for the exchanged closed string, analogous to the BFKL kernel at weak coupling, with diffusing taking place in  $\log(k_\perp)$ , the virtuality of the off-shell gluon dipole.  $\mathcal{D} = 2/\sqrt{\lambda}$  at strong coupling, compared to  $\mathcal{D} = 7\zeta(3)\lambda/2\pi^2$  in weak coupling.

**Fit to HERA Data:** To confront data at HERA, it is necessary to face the issue of confinement and saturation. Confinement can be addressed via a hardwall cutoff,  $z < z_0$ , or via a softwall model, which we shall return to shortly. The effect of saturation can next be included via the  $AdS_3$  eikonal representation.

To extract the key feature of holographic treatment, we shall first adopt a simplifying assumption. We note that both integrals in  $z$  and  $z'$  in (2), are sharply peaked, the first around  $z \sim 1/Q$  and the second around the inverse proton mass,  $z' \equiv 1/Q' \sim 1/m_p$ . To gain an understanding on the key features of dual approach, it is sufficient to approximate both integrand by delta functions. Under such an ‘‘ultra-local’’ approximation, all structure functions take on very simple form, e.g,

$$F_2(x, Q^2) = \frac{g_0^2}{8\pi^2 \lambda} \frac{Q}{Q'} \frac{e^{(j_0 - 1)\tau}}{\sqrt{\pi \mathcal{D} \tau}} e^{-(\log Q - \log Q')^2 / \mathcal{D} \tau} + \text{Confining Images}, \quad (4)$$

with diffusion time given more precisely as  $\tau = \log(s/QQ'\sqrt{\lambda}) = \log(1/x) - \log(\sqrt{\lambda}Q'/Q)$ . Here the first term is conformal. To incorporate confinement, we consider first the hardwall model. The confining effect can be expressed in terms of image charges [3]. It is important to note, with or without confinement, the amplitude corresponding to (4) grows asymptotically as  $(1/x)^{j_0 - 1} \sim s^{j_0 - 1}$ , thus violating the Froissart unitarity bound at very high energies. The eikonal approximation in  $AdS$  space, (2), restores unitarity via multi-Pomeron shadowing [8, 4, 9].

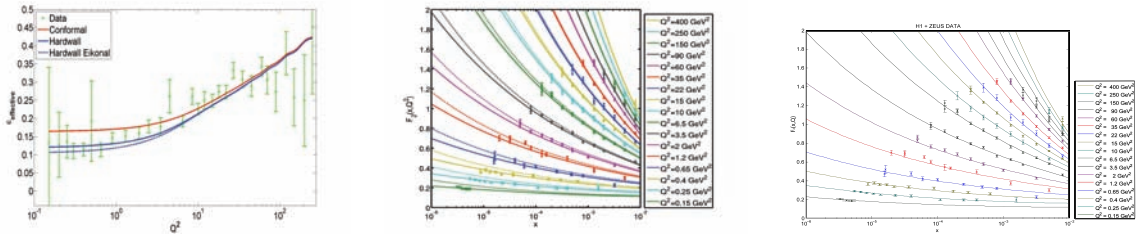


**Figure 2:** In the left, (a), with the BPST Pomeron intercept at 1.22,  $Q^2$  dependence for ‘‘effective intercept’’ is shown for conformal, hardwall and hardwall eikonal model. In the center, (b), a more detailed fit is presented contrasting the fits to HERA data at small  $x$  by a single hardwall Pomeron vs hardwall eikonal respectively. The softwall model, (c), was also used to fit the  $F_2$  proton structure function, (c), to the right, with good success.

We show in Fig. 2 various comparisons of our results [10] to the small- $x$  DIS data from the combined H1 and ZEUS experiments at HERA [7]. Both the conformal, the hard-wall model, soft-wall, as well as

the eikonized hard-wall model can fit the data reasonably well. This can best be seen in Fig. 2a to the left which exhibits the  $Q^2$  dependence of an effective Pomeron intercept. This can be understood as a consequence of diffusion. However, it is important to observe that the hard-wall model provides a much better fit than the conformal result for  $Q^2$  less than the transition scale,  $Q_c \sim 2 \sim 3 \text{ GeV}^2$ . The best fit to data is obtained using the hard-wall eikonal model, with a  $\chi^2 = 1.04$ . This is clearly shown by Fig. 2b, where we present a comparison of the relative importance of confinement versus eikonal at the current energies. (For more details, see Ref. [10].)

**Confinement and Softwall:** It is clear that, for  $Q^2$  small, confinement is important. We find that confinement effect persists at an increasingly large value of  $Q^2$  as  $1/x$  increases. Equally important is the fact that the transition scale  $Q_c^2(x)$  from conformal to confinement increases with  $1/x$ , and it comes before saturation effect becomes important. Therefore the physics of saturation should be discussed in a confining setting <sup>2</sup>.

In order to test the generality of this observation, as well as other considerations, we turn next to a brief discussion on the use of softwall model. The soft wall model was proposed as a holographic approach [19] leading to linear meson trajectories <sup>3</sup>. For our purpose, it is sufficient to focus on graviton fluctuations and we shall simply treat this as a purely geometric confinement model <sup>4</sup>.

In the softwall model, the graviton dynamics involve a spin dependent mass-like term  $\alpha^2(j) = 2\sqrt{\lambda}(j - j_0)$ . Pomeron exchange corresponds to infinite set of Regge exchanges, labelled by  $t_n = \Lambda^2(4n + 2\alpha + 2 - 2c + (2\alpha^2/3 - 3/8))$  and the corresponding propagator can be written as combination of Whittaker's functions and their Wronskian

$$\chi_P(j, z, z', t) = \frac{M_{\kappa, \mu}(z_{<})W_{\kappa, \mu}(z_{>})}{W(M_{\kappa, \mu}, W_{\kappa, \mu})} \quad (5)$$

for  $\kappa = \kappa(t)$  and  $\mu = \mu(j)$ .  $\Lambda$  controls the strength of the soft wall and in the limit  $\Lambda \rightarrow 0$  one recovers the conformal solution, i.e., that in (4).

A softwall model also fits HERA data well, as shown in Fig. 2c, to the right. We provide in Table-1 a comparative quantitative analysis for various options. The fit using softwall treatment was done with the same methods used previously for the conformal and hardwall models in [10], making the results directly comparable.

Model	$\rho$	$g_0^2$	$z_0$ (GeV <sup>-1</sup> )	$Q'$ (GeV)	$\chi_{dof}^2$
conformal	$0.774^* \pm 0.0103$	$110.13^* \pm 1.93$	-	$0.5575^* \pm 0.0432$	11.7 (0.75*)
hard wall	$0.7792 \pm 0.0034$	$103.14 \pm 1.68$	$4.96 \pm 0.14$	$0.4333 \pm 0.0243$	1.07 (0.69*)
softwall	0.7774	108.3616	8.1798	0.4014	1.1035

**Table 1:** Comparison of the best fit values for the conformal, hard wall, and softwall models.

If we look at the energy dependence of the Pomeron propagator, we can see a softened behavior in the regge limit. In the forward limit,  $t = 0$ , the conformal amplitude scales as  $-s^{\alpha_0} \log^{-1/2}(s)$ , but

<sup>2</sup>This has been stressed in [10]. In contrast, conventional treatment, e.g., color-glass condensate, assumes that saturation scale can be understood perturbatively.

<sup>3</sup>Several dynamical softwall toy models, where the confinement is due to a non-trivial dilaton field, have subsequently been constructed. See various references cited in [19]

<sup>4</sup>For our present purpose, we replace  $A$  in (1) by  $c(\Lambda z)^2/3 - \log(z/R)$ , with  $c = \pm 1$ . The choice for  $c$  remains a source of debate, [20]. For this analysis, we shall keep  $c = -1$ , as originally done in [19]. The possibility of  $c = +1$  will be addressed elsewhere.

this behavior is softened to  $-s^{\alpha_0} \log^{-3/2}(s)$  in the hardwall and softwall models. This corresponds to the softening of a  $j$ -plane singularity from  $1/\sqrt{j-j_0} \rightarrow \sqrt{j-j_0}$ . This observation is generic to all confining scenarios, and its consequences will be explored further elsewhere.

**Pomeron Intercept, DGLAP Connection, and Anomalous Dimensions:** Let us examine briefly the concept of a BPST Pomeron in more general context of conformal field theories (CFT). A CFT 4-point correlation function  $\mathcal{A} = \langle \phi(x_1)\phi(x_2)\phi(x_3)\phi(x_4) \rangle$  can be analyzed in an operator product expansion (OPE) by summing over allowed primary operators  $\mathcal{O}_{k,j}$ , with integral spin  $j$  and dimensions  $\Delta_k(j)$ , and their descendants. due to interaction, these conformal dimensions differ from their canonical dimension, with  $\gamma_k(j) = \Delta_k(j) - j - \tau_k$ , with twist  $\tau_k$ .

Consider next the moments for the structure function  $F_2, M_n(Q^2) = \int dx x^{n-2} F_2(x, Q^2)$ . From OPE[18], or, equivalently DGLAP evolution,

$$M_n(Q^2) \rightarrow Q^{-\gamma(n)} \quad (6)$$

where  $\gamma(n)$  is the anomalous dimension for the twist-two operators, appropriate for DIS. In particular,  $\gamma_2 = 0$ , due to energy-momentum conservation. In our dual treatment, it is possible to identify  $\gamma_n$  by our ‘‘dimension-spin’’ curve,  $\Delta(j)$ , with  $\gamma(n) = \Delta(n) - n - 2$ . At  $j = 2$ , the lowest twist-2 operator is the dimension-4 energy-momentum tensor which assures  $\gamma_2 = 0$ .

More generally, it was shown in [3] that  $\Delta(j)$  is analytic in  $j$ , so that one can expand  $\Delta(j)$  about  $j = 2$  as  $\Delta(j) = 4 + \alpha_1(\lambda)(j-2) + O_G((j-2)^2)$ , with the coefficient  $\alpha_1(\lambda) = \sqrt{\lambda}/4 + O(1)$ . It was also stressed in [3, 17] that the  $\Delta - j$  curve must be symmetric about  $\Delta = 2$  due to conformal invariance, and, by inverting  $\Delta(j)$ , one has  $j(\Delta) = j(2) + \alpha_1(\lambda)^{-1}(\Delta - 2)^2 + \dots$ . At large  $\lambda$ , the curve  $j(\Delta)$  is parabolic around its minimum at  $\Delta = 2$  and constrained by  $j(4) = 2$ , as exhibited in Fig. 1b.

The Pomeron intercept is simply the minimum of  $j(\Delta)$  curve at  $\Delta = 2$ , that is,  $j_0 = j(2)$ . In particular, it admits an expansion in  $1/\sqrt{\lambda}$ . In a systematic expansion [21, 17], one finds that  $\alpha_P = 2 - \frac{2}{\lambda^{1/2}} - \frac{1}{\lambda} + \frac{1}{4\lambda^{3/2}} + \frac{6\zeta(3)+2}{\lambda^2} + \dots$ , where terms upto  $1/\lambda^3$  have been found. A similar analysis also leads to systematic expansion for the Odderon intercepts in  $1/\sqrt{\lambda}$ . As explained in [5, 17], there are at least two leading odderon trajectories. One has an expansion

$$\alpha_{O,a} = 1 - \frac{8}{\lambda^{1/2}} - \frac{4}{\lambda} + \frac{13}{\lambda^{3/2}} + \frac{96\zeta(3)+41}{\lambda^2} + \frac{288\zeta(3)+\frac{1249}{16}}{\lambda^{5/2}} + \frac{-720\zeta(5)+192\zeta(3)+\frac{159}{4}}{\lambda^3} + \dots$$

Interestingly, the second trajectory, remains at  $\alpha_{O,b} = 1$ , independent of  $\lambda$ .

**Discussion:** We have presented the phenomenological application of the AdS/CFT correspondence to the study of DIS at small  $x$ , demonstrating the usefulness of the strong coupling BPST Graviton/Pomeron. Encouraged by this, we plan to undertake a fuller study of several closely related diffractive process: total and elastic cross sections, DIS, virtual photon production and double diffraction production of heavy quarks, etc. The goal is that by over-constraining the basic AdS building blocks of diffractive scattering, this framework will give a compelling phenomenology prediction for the double diffractive production of glueballs, Higgs, etc., to aid in the analysis of LHC data.

**Acknowledgments:** The work of RCB was supported by the Department of Energy under contract DE-FG02-91ER40676, that of TR and CIT by the Department of Energy under contract DE-FG02-91ER40688, Task-A, and that of MD by FCT project CERN/FP/116358/2010.

## References

- [1] J. M. Maldacena, *Adv. Theor. Math. Phys.* **2**, 231 (1998), [arXiv:hep-th/9711200].
- [2] E. Witten, *Adv. Theor. Math. Phys.* **2**, 253-291 (1998), [hep-th/9802150].
- [3] R. C. Brower, J. Polchinski, M. J. Strassler and C-I Tan, *JHEP* **0712**, 005 (2007), [hep-th/0603115].
- [4] R. C. Brower, M. J. Strassler and C-I Tan, *JHEP* **0903**, 092 (2009), [arXiv:0710.4378 [hep-th]].
- [5] R. C. Brower, M. Djuric and C-I Tan, *JHEP* **0907**, 063 (2009), [arXiv:0812.0354 [hep-th]].
- [6] E. Avsar, Y. Hatta and T. Matsuo, *JHEP* **1003**, 037 (2010), [arXiv:0912.3806 [hep-th]].
- [7] F. D. Aaron *et al.* [H1 and ZEUS Collaboration], *JHEP* **1001**, 109 (2010), [arXiv:0911.0884 [hep-ex]].
- [8] R. C. Brower, M. J. Strassler and C-I Tan, *JHEP* **0903**, 050 (2009), [arXiv:0707.2408 [hep-th]].
- [9] L. Cornalba, M. S. Costa, J. Penedones, R. Schiappa, *Nucl. Phys.* **B767**, 327-351 (2007), [hep-th/0611123].  
L. Cornalba, M. S. Costa, J. Penedones, *JHEP* **0806**, 048 (2008), [arXiv:0801.3002 [hep-th]].
- [10] R. C. Brower, M. Djuric, I. Sarcevic and C-I Tan, *JHEP* **1011**, 051 (2010), [arXiv:1007.2259 [hep-ph]].
- [11] L. Cornalba, M. S. Costa, J. Penedones, *Phys. Rev. Lett.* **105**, 072003 (2010).
- [12] R. Nishio and T. Watari, *Phys. Rev. D* **84**, 075025 (2011), [arXiv:1105.2999 [hep-ph]]; *Phys. Lett. B* **707**, 362 (2012), [arXiv:1105.2907 [hep-ph]]; *Phys. Rev. D* **90**, no. 12, 125001 (2014).
- [13] A. Watanabe and K. Suzuki, *Phys. Rev. D* **86**, 035011 (2012), [arXiv:1206.0910 [hep-ph]]; *Phys. Rev. D* **89**, no. 11, 115015 (2014), [arXiv:1312.7114 [hep-ph]]; A. Watanabe and H. n. Li, arXiv:1502.03894 [hep-ph].
- [14] M. S. Costa and M. Djuric, *Phys. Rev. D* **86**, 016009 (2012), [arXiv:1201.1307 [hep-th]]; *JHEP* **1309**, 084 (2013) [arXiv:1307.0009 [hep-ph]].
- [15] R. C. Brower, M. Djuric and C. I. Tan, *JHEP* **1209**, 097 (2012), [arXiv:1202.4953 [hep-ph]]; *Int. J. Mod. Phys. A* **29**, no. 28, 1446013 (2014).
- [16] Y. Hatta, E. Iancu and A. H. Mueller, *JHEP* **0801**, 026 (2008) J. L. Albacete, Y. V. Kovchegov, A. Taliotis, *JHEP* **0807**, 074 (2008); Y. V. Kovchegov, Z. Lu, A. H. Rezaeian, *Phys. Rev.* **D80**, 074023 (2009). E. Levin, I. Potashnikova, *JHEP* **1008**, 112 (2010).
- [17] R. C. Brower, M. S. Costa, M. Djuric, T. Raben and C. I. Tan, *JHEP* **1502**, 104 (2015) [arXiv:1409.2730].
- [18] J. Polchinski, M. J. Strassler, *JHEP* **0305**, 012 (2003). [hep-th/0209211].
- [19] A. Karch, E. Katz, D. T. Son and M. A. Stephanov, *Phys. Rev. D* **74**, 015005 (2006), [hep-ph/0602229]; B. Batell and T. Gherghetta, *Phys. Rev. D* **78**, 026002 (2008), [arXiv:0801.4383 [hep-ph]]; E. Katz, A. Lewandowski and M. D. Schwartz, *Phys. Rev. D* **74**, 086004 (2006) [hep-ph/0510388].
- [20] A. Karch, E. Katz, D. T. Son and M. A. Stephanov, *JHEP* **1104**, 066 (2011), [arXiv:1012.4813 [hep-ph]]; G. F. de Teramond and S. J. Brodsky, *Nucl. Phys. Proc. Suppl.* **199**, 89 (2010) [arXiv:0909.3900 [hep-ph]].
- [21] B. Basso, arXiv:1109.3154 [hep-th]; M. S. Costa, V. Goncalves and J. Penedones, *JHEP* **1212**, 091 (2012); [arXiv:1209.4355 [hep-th]]; A. V. Kotikov and L. N. Lipatov, *Nucl. Phys. B* **874**, 889 (2013); [arXiv:1301.0882 [hep-th]]; N. Gromov, F. Levkovich-Maslyuk, G. Sizov and S. Valatka, *JHEP* **1407**, 156 (2014) [arXiv:1402.0871 [hep-th]];